Full Title: Co-immunoprecipitation with MYR1 identifies three additional proteins within the *Toxoplasma* parasitophorous vacuole required for translocation of dense granule effectors into host cells

Running Title: Novel proteins required for *Toxoplasma* effector export

Alicja M. Cygan[a*], Terence C. Theisen[a*], Alma G. Mendoza[a], Nicole D. Marino[a,b], Michael W. Panas[a], and John C. Boothroyd[a,#]

Author Affiliations:

[a]Department of Microbiology and Immunology, Stanford School of Medicine, Stanford CA, USA

[b]Current address: Department of Microbiology and Immunology, University of California, San Francisco CA, USA

[*] A.M.C. and T.C.T. contributed equally to this work. A.M.C. took the lead on writing the manuscript.

[#]Address correspondence to John C. Boothroyd, jboothr@stanford.edu

Word count, abstract: 177

Word count, text: 4,236

Abstract

Toxoplasma gondii is a ubiquitous, intracellular protozoan that extensively modifies infected host cells through secreted effector proteins. Many such effectors must be translocated across the parasitophorous vacuole (PV) in which the parasites replicate, ultimately ending up in the host cytosol or nucleus. This translocation has previously been shown to be dependent on five parasite proteins: MYR1, MYR2, MYR3, ROP17, and ASP5. We report here the identification of several MYR1-interacting and novel PV-localized proteins via affinity purification of MYR1, including TGGT1_211460 (dubbed MYR4), TGGT1_204340 (dubbed GRA54) and TGGT1_270320 (PPM3C). Further, we show that three of the MYR1-interacting proteins, GRA44, GRA45, and MYR4, are essential for the translocation of the *Toxoplasma* effector protein GRA16, and for the upregulation of human c-Myc and cyclin E1 in infected cells. GRA44 and GRA45 contain ASP5-processing motifs, but like MYR1, processing at these sites appears to be nonessential for their role in protein translocation. These results expand our understanding of the mechanism of effector translocation in *Toxoplasma* and indicate that the process is highly complex and dependent on at least eight discrete proteins.

Importance

Toxoplasma is an extremely successful intracellular parasite and important human pathogen. Upon infection of a new cell, *Toxoplasma* establishes a replicative vacuole and translocates parasite effectors across this vacuole to function from the host cytosol and nucleus. These effectors play a key role in parasite virulence. The work reported here newly identifies three parasite proteins that are necessary for protein translocation into the host cell. These results significantly increase our knowledge of the molecular players involved in protein translocation in *Toxoplasma*-infected cells, and provide additional potential drug targets.

Introduction

Toxoplasma gondii is an obligate intracellular parasite that can cause severe illness in immunocompromised individuals and the developing fetus. It is estimated to infect up to a third of the world's population, and has an unparalleled host range, infecting virtually any nucleated cell in almost any warm-blooded animal (1). In order to survive within a host cell, *Toxoplasma* tachyzoites, the rapidly-dividing, asexual stage of the parasite, establish a replicative niche, the parasitophorous vacuole (PV), whose membrane (PVM) acts as the interface between parasite and host. While the PV protects intracellular *Toxoplasma* from clearance by the innate immune system, it also acts as a barrier that *Toxoplasma* must overcome in order to hijack host resources.

Toxoplasma extensively modifies the host cells it infects via secreted effectors, either rhoptry (ROP) or dense granule (GRA) proteins, which it introduces into the host during or following invasion (2). In recent years, several *Toxoplasma* GRAs, including GRA16, GRA24, IST, HCE1/TEEGR, GRA28, and GRA18, have been identified that are translocated across the PVM into the host cell cytosol and/or nucleus, where they can have profound effects on host processes (3–9). The machinery that is responsible for the translocation of these effectors across the *Toxoplasma* PVM is incompletely defined. A recent forward genetic screen identified several parasite proteins essential for GRA protein translocation, including MYR1, MYR2, MYR3, (named for their effect on host c-Myc regulation) and the rhoptry-derived protein kinase, ROP17 (10–12). Precisely how these proteins function to promote protein translocation across the PVM is poorly understood. Of the four, the only protein with a known biochemical function is

ROP17, a serine/threonine protein kinase that phosphorylates host, and perhaps parasite proteins at the PVM (6, 13, 14).

In addition to MYR1, MYR2, MYR3, and ROP17, an active *Toxoplasma* aspartyl protease V (ASP5), which proteolytically processes secreted proteins at the amino acid sequence "RRL" (also known as a *Toxoplasma* export element, or TEXEL), is also required for the translocation of all exported GRAs studied thus far (5, 6, 8, 9, 15–17). In *Plasmodium*, the homolog of ASP5, plasmepsin V, appears to "license" many proteins for export across the PVM by proteolytically processing them at a *Plasmodium* export element ("RxLxE/Q/D") (18–21). Intriguingly, and as for *Plasmodium* (22, 23), not all of *Toxoplasma's* exported GRAs contain "RRL" motifs (e.g. GRA24, GRA28, and HCE1/TEEGR lack such an element), which leaves open the possibility that ASP5's role in translocation is in processing the translocation machinery, rather than the effectors themselves. Indeed, MYR1 is processed by ASP5, but this processing is not necessary for protein export, as unprocessed full length MYR1 harboring a mutated "RRL" motif can still promote the translocation of the effector GRA24 to the host nucleus (24). The role of ASP5 processing of MYR1, therefore, remains unknown.

To learn more about the mechanism of protein translocation in *Toxoplasma*, and to complement the genetic approaches taken previously, we report here the use of MYR1 as "bait" for immunoprecipitation followed by mass spectrometry (IP-MS) to identify putative MYR1-associated proteins that are involved in effector translocation. Of the many associating proteins, at least eleven are shown here or were previously known to be PV-localized and, of these, three additional proteins are now shown to be required for GRA translocation across the PVM. Interestingly, all three of these new components

96 contain “RRL” motifs, with two confirmed to be cleaved in an ASP5-depndent manner;
97 yet, like MYR1, cleavage at these sites appears not to be required for their translocation
98 function. Thus, we have expanded the list of proteins involved in GRA translocation to
99 eight while also expanding the enigma of why at least three of these components are
100 proteolytically processed without any apparent impact on their one known function.
101

Results

We previously reported the use of a forward genetic screen to identify *Toxoplasma* genes required for the induction of human c-Myc. This identified *MYR1*, *MYR2*, *MYR3*, and *ROP17* as essential for the translocation of effector proteins across the PVM (10–12). Two of these proteins, MYR1 and MYR3, were found to co-precipitate with each other (11), and we hypothesized that MYR1 functions in complex with other yet unidentified proteins to facilitate effector translocation across the PVM. Given the small but significant reduction in plaque size observed when growing strains deleted in MYR1, MYR2, and MYR3 on human foreskin fibroblasts (HFFs) (11), we also reasoned that the genetic approach might also miss genes whose disruption substantially reduces fitness.

To identify additional MYR1-associating proteins, therefore, we adopted a biochemical approach. Specifically, we immunoprecipitated 3xHA-tagged MYR1 from HFFs infected for 24 hours with an RH::*MYR1-3xHA* strain, or from an untagged RH strain to control for proteins that co-precipitate with the anti-HA beads nonspecifically (**Fig. 1A**). Liquid chromatography-tandem mass spectrometry (LC-MS/MS) was performed on the eluates and the identified parasite proteins were ranked by the ratio of average normalized spectral abundance factors (NSAFs) for a given protein in the RH:*MYR1-3xHA* lysates compared to the RH control (25). This mass spectrometry experiment was performed twice (IP 1 and IP 2). As expected, MYR1 was the most enriched protein in both biological replicates (**Fig. 1B**). Additionally, several PV- or PVM-localized GRA proteins were highly enriched (enrichment score >10) in the MYR1-3xHA immunoprecipitations over the untagged RH control, including GRA44, CST1,

GRA52, MAG1, PPM11C, GRA50, MAF1a, GRA7, and a GRA12 paralog, in addition to two exported effector proteins, GRA16 and GRA28, of which GRA16 has been shown to be exported in a MYR1-dependent manner (10) (**Fig. 1B, File S1**). The large number of enriched PV- and PVM-localized proteins may be explained by the mild detergent conditions used (0.1% NP-40), which were chosen in an attempt to maintain associating proteins, although these proteins might also be associating with one another in large, non-specific complexes or lipid rafts (26).

Importantly, and also as expected, the known MYR1-associating protein, MYR3, was enriched in the MYR1-3xHA immunoprecipitations, albeit with an enrichment score (4.5) that did not put it in the top 20 most enriched proteins (**Fig. 1B, File S1**). Of note, ROP17 was not substantially enriched (enrichment score = 1.2) and no peptides for MYR2 were detected, but neither protein has previously been found to associate with MYR1 and so this was not unexpected. Human proteins with an enrichment score >10 include Filamin-C (FLNC), DNA-dependent protein kinase catalytic subunit (PRKDC), sarcoplasmic/endoplasmic reticulum calcium ATPase 2 (ATP2A2), and Alpha-N-acetylglucosaminidase (NAGLU) (**File S1**). As our focus was on parasite proteins only, the potential role of these human proteins in *Toxoplasma* infection was not further investigated.

To screen for a possible role in GRA effector translocation, we focused on the top 6 most enriched parasite proteins: GRA44 (TGGT1_228170), CST1 (TGGT1_264660), TGGT1_204340, TGGT1_211460, PPM3C (TGGT1_270320), and GRA52 (TGGT1_319340). GRA45 (TGGT1_316250) was also pursued because it is a known binding partner of the top hit, GRA44 (27), and it also had a substantial

148 enrichment score of 5.2 in the immunoprecipitations (**Fig. 1B**). Interestingly, two well-
149 characterized PV proteins that have not previously been described to be involved in
150 effector translocation, GRA7 (TGGT1_203310) and MAF1a (TGGT1_279100), were
151 substantially enriched and, since antibodies and gene knockouts for both were readily
152 available, we included these in the list of genes to explore further. Lastly, as a positive
153 control for a protein whose disruption is known to prevent effector translocation, we also
154 included MYR3 in the pipeline for gene disruption and testing. All ten proteins chosen
155 for further analysis are highlighted in orange in Fig. 1B.

156 With the exception of ASP5, and as might be expected, all proteins so far
157 published as required for effector translocation across the PVM localize to the PV/PVM
158 (2). Of the ten proteins chosen for further analysis, GRA44, GRA45, CST1, GRA7,
159 GRA52, and MAF1a, are all known to be PV/PVM-localized (27–31). The localization of
160 211460 and PPM3C has not been reported, but both include predicted signal peptides
161 (see below) as does 204340 which has been described as possibly micronemal (32).
162 We therefore set out to localize these three proteins within infected cells. To do this, we
163 generated populations of parasites in which each of the three genes was endogenously
164 modified to encode a 3xHA-tag immediately before the stop codon and then assessed
165 the protein's localization by immunofluorescence assay (IFA). Correct integration of the
166 3xHA-tag into the appropriate locus was confirmed by PCR and by checking for an
167 appropriately sized HA-tagged protein via western blotting. The results (**Fig. 2A**)
168 showed major bands at ~130 kDa, ~110 kDa, and ~70 kDa for 211460, 204340, and
169 PPM3C, respectively. In the case of 204340 and PPM3C, this is close to the predicted
170 sizes of ~97 kDa and ~60kDa (ToxoDB v45). For 211460, however, the mobility is

171 significantly retarded relative to its predicted size of ~100 kDa. This could be due to its
172 acidic pI of 4.91 (ToxoDB v45) which is known to reduce protein mobility on SDS-PAGE
173 (33), and/or to post-translational modifications (all three proteins are reported to be
174 phosphorylated (31; ToxoDB v45)). This same slower-than-expected mobility for the
175 major band was seen for an independently generated, cloned line expressing HA-
176 tagged 211460 (**Fig. S1A**) and so we conclude that this is the correct mobility for this
177 protein. Interestingly, both the 211460-3xHA tagged population and single clone also
178 showed a smaller but considerably weaker band at around the expected size (~100
179 kDa). Whether this smaller MYR4 product is biologically relevant, or is simply a product
180 of protein degradation, is unclear.
181 Using the HA-tagged 211460, 204340, and PPM3C parasite populations, we next
182 sought to determine the localization of these proteins in infected cells. Using SignalP
183 software (v5.0), all three proteins have strongly predicted signal peptides although in the
184 case of 211460, this is only true if translation starts at the fourth in-frame methionine
185 (position 61) relative to the protein sequence predicted on ToxoDB (v45). The results
186 (**Fig. 2B**) show a clear PV-like signal outside of the parasites in the 211460-3xHA,
187 204340-4xHA, and PPM3C-3xHA populations, including at the periphery of the PV. The
188 PV-localization for 211460 is further confirmed in the independently generated clonal
189 line (**Fig. S1B**). Thus, we conclude that 211460, 204340, and PPM3C are at least
190 transiently localized to the *Toxoplasma* PV during infection. Furthermore, we also
191 assessed the localization of these proteins within the parasites themselves. The results
192 (**Fig. S2**) show that while PPM3C appears to be present throughout the parasite,
193 211460 and 204340 show a clear, punctate staining pattern that largely co-localizes

194 with the dense granule protein GRA7, suggesting that these two proteins are also GRA
195 proteins. We therefore designate *204340* as *GRA54* for its GRA-like localization, and
196 *211460* as *MYR4*, for reasons described below.

197 To assess their potential involvement in GRA effector translocation, we
198 attempted to generate knockouts of our candidate genes in a strain of *Toxoplasma* that
199 constitutively expresses an HA-tagged version of the MYR1-dependent secreted
200 effector protein GRA16, RHΔ*gra16*::GRA16-HA ("parental"). To do this, we co-
201 transfected a CRISPR/Cas9 sgRNA plasmid that targets the first exon of the relevant
202 gene along with a pTKO2-CAT-mCherry plasmid (CAT encodes the chloramphenicol-
203 resistance gene, chloramphenicol acetyl transferase; **Fig. 3A**). Following selection with
204 chloramphenicol, we cloned the populations by limiting dilution and confirmed disruptive
205 integration of the vector by PCR with gene-specific primers. Using this strategy, we
206 were able to disrupt the genomic loci of *MYR3*, *GRA44*, *GRA45*, *CST1*, *GRA54*, *MYR4*,
207 *PPM3C*, and *GRA7* (**Fig. S3**). Despite several attempts, however, we were unable to
208 generate a *GRA52* mutant. This gene may be essential as it has a very negative
209 CRISPR fitness score of -3.96 (35). Given that the *MAF1* locus is expanded in
210 *Toxoplasma*, with 4 copies in RH parasites (36), we chose not to attempt a
211 CRISPR/Cas9 approach to knockout MAF1a, and instead utilized a previously
212 generated strain in which the entire *MAF1* cluster (including MAF1a and MAF1b) is
213 deleted (31).

214 To determine if the absence of any of the candidate genes results in a defect in
215 effector translocation across the PVM, we used IFA to assess both GRA16-HA export to
216 the host nucleus and host c-Myc upregulation (which *Toxoplasma* induces during

infection (37)) in the disrupted lines. Quantified results for all nine genes tested show that disruption of *GRA44*, *GRA45*, *MYR4* and the previously described *MYR3*, all resulted in a complete or near-complete block in GRA16 export to the host nucleus (**Figs. 3B, S4**) and a failure to upregulate host c-Myc (**Figs. 3C, S4**); on the other hand, disruption of *GRA7*, *CST1*, *GRA54*, or *PPM3C* resulted in no detectable effect on either of these two phenotypes. Additionally, we found that the previously generated Δ*maf1* strain also had normal GRA16 export to the host nucleus (**Fig. 3D**). These results indicate that of the nine genes tested here, only *MYR3*, *GRA44*, *GRA45* and *MYR4* are necessary for the translocation of GRA effectors across the PVM.

To test the generality of their role in effector translocation, we next assessed the impact of these gene disruptions on the upregulation of host cyclin E1 which has been shown to be dependent on export of the MYR1-dependent effector HCE1/TEEGR (6). The results showed that, as for GRA16, disruption of *MYR3*, *GRA44*, *GRA45*, and *MYR4* also resulted in a block in cyclin E1 upregulation in infected host cells, while no obvious defect was observed in the parasite lines disrupted in *GRA7*, *CST1, GRA54* and *PPM3C* (**Fig. 3E**). A repetition of the cyclin E1 western blot with higher parasite input reveals that the absence of cyclin E1 upregulation observed in Δ*gra44* parasites in Fig. 3E is not due to low parasite input in that particular experiment (**Fig. S5**). These results argue that *GRA44*, *GRA45* and *MYR4* are all required for translocation across the PVM of at least two independent GRA effectors.

Our previous work has shown that deletion of *MYR1*, *MYR2*, and *MYR3* results in a small but significant, negative effect on parasite growth *in vitro* (11). To determine if disruption of the three new genes involved in effector translocation described here has a

similar impact, we infected HFF monolayers with each of the disrupted lines, fixed the monolayers 7 days post infection, and measured plaque size. The results show that the Δ*myr4,* Δ*gra44* and Δ*gra45* strains all exhibit a significant growth defect compared to the parental strain (**Fig. 3F**). We did not test for rescue of the growth phenotype with complementation due to limitations in selectable markers available in these strains. The Δ*gra54* and Δ*ppm3c* strains, on the other hand, did not have significant growth defects, consistent with the growth defects observed being dependent on the respective genotype rather than nonspecific effects of the manipulations.

To confirm that ablation of *GRA44*, *GRA45*, and *MYR4* loci are responsible for the observed defect in GRA16 export, we transiently expressed a C-terminally V5-tagged version of each protein, driven by its native promoter, in the relevant disrupted line. These transiently transfected parasites were then assessed for GRA16-HA export to the host nucleus via IFA. The results showed that the parental and complemented strains had GRA16-HA signal in both the vacuole and host nucleus, while the parasites within the population that did not express the complementing transgene (as indicated by lack of anti-V5 staining) showed essentially no GRA16 in the host nucleus (**Figs. 4A, 4B**). Thus *GRA44*, *GRA45*, and *MYR4* are indeed essential for the translocation of effectors across the PVM, and we therefore designate *211460* as *MYR4,* consistent with previous nomenclature (10, 11).

Interestingly, GRA44, GRA45 and MYR4 all contain one or two instances of the three-amino-acid motif “RRL” (**Fig. 5A**), which has previously been shown to be the preferred sequence for cleavage by ASP5 protease (15). Indeed, cleavage at the three sites shown in GRA44 and GRA45 (27), as well as at the first “RRL” motif in the

secreted GRA effector, GRA16 (15), has been experimentally confirmed. ASP5 is essential for the translocation of all GRA effectors so far tested (5, 6, 8, 9, 15–17) and it has previously been suggested that ASP5-mediated cleavage of some effectors is required to "license" them for translocation across the PVM, as appears to be the case in *Plasmodium* (38, 39). Given, however, that not all such effectors contain ASP5 processing motifs (e.g., GRA24 lacks the canonical "RRL" and shows no evidence of ASP5-dependent processing; (17)), and given that the three newly identified components of the translocation machinery identified here do, we hypothesized that ASP5's essential contribution to effector translocation across the PVM might be in processing one or more components of the translocation machinery. We have previously shown that MYR1 is also processed by ASP5 at a "RRL" site but this does not appear to be required for MYR1 to function in effector translocation (24) and so we turned our attention to the newly identified translocation components identified here.

To determine if processing at the "RRL" sites of GRA44, GRA45, and MYR4 is required for protein translocation activity, we mutated the ASP5 cleavage sites by converting the first arginine to an alanine (i.e., RRL→ARL) in the V5-tagged complementation plasmids for each gene, and transiently transfected these into the corresponding disrupted line. Western blots were then used to show that processing of GRA45 at its lone "RRL" and of GRA44 at its second "RRL" is indeed abrogated by the mutations (**Fig. 5B**). For the more N-terminal site in GRA44 (R83A), we cannot definitively confirm that the mutation abrogates ASP5 processing because GRA44 is epitope-tagged at its C-terminus and so, assuming cleavage at the two sites is an independent event, cleavage at the downstream site will produce a C-terminal, V5-

tagged fragment whether or not cleavage occurs at R83A. We fully expect, however, that the RRL→ARL change disrupts ASP5 cleavage at this site because it did in the two other examples shown here (GRA45 and the downstream site in GRA44, R1348A) and because RRL→ARL mutations have previously been shown to disrupt the ASP5-dependent cleavage of other proteins (24, 27).

Interestingly, mutation of the "RRL" to an "ARL" in MYR4 did not appear to affect the processing of the protein (**Fig. 5B**). To rule out whether this is due to incomplete ablation of the ASP5 processing site with a single amino acid substitution, we assessed the processing of an RRL→AAA MYR4 mutant where the entire ASP5-processing motif is mutated to alanines. The results (**Fig. 5C**) show that the higher molecular weight product of MYR4 (~130kD) does not change in mobility upon mutation of the entire "RRL" motif, and thus we conclude that little if any MYR4 is processed by ASP5. Note that, despite repeated attempts with large amounts of DNA, the signal for the transiently expressed MYR4 was never strong enough to confidently conclude whether a small amount of a processed form might be present in these transiently transfected parasites; we therefore cannot comment on whether the low-intensity, smaller molecular weight product of MYR4 (~100kD) seen in long exposures of endogenously tagged wild type MYR4 (**Figs. 2A, S1A**) is a result of an ASP5 processing event.

Having generated the four RRL→ARL mutants, and having validated that ASP5 cleavage is ablated in at least two instances, we next tested each for its impact on the localization of the epitope-tagged, C-terminal portion of the protein and on the ability of the uncleaved protein to function; i.e., whether it can rescue the defect in effector protein translocation. The results show that the RRL→ARL mutated versions of each

309 protein are still secreted into the PV, similar to the wild type copy (**Figs. 6A, 4A**), and
310 are all able to rescue the translocation defect to a similar extent as the corresponding
311 control (WT) plasmid (**Fig. 6B**). While the GRA45 R64A mutant did substantially rescue
312 translocation, it did not consistently rescue to wildtype levels. Nevertheless, these data
313 suggest that mutation of the “RRL” sites in GRA44, GRA45, and MYR4 to “ARL” does
314 not substantially affect their function in effector protein translocation.

Discussion

Using affinity purification of MYR1 under conditions expected to retain associating partners, we identify three novel parasite proteins, GRA44, GRA45, and MYR4, as essential for the export of GRA effectors into infected cells. Additionally, we localize MYR4, as well as two additional MYR1-associating proteins, GRA54 and PPM3C, to the PV in infected cells. Altogether, eight proteins are now known to be necessary for effector export: the 3 described here and MYR1*,* MYR2*,* MYR3*,* ROP17 and ASP5 – summarized in Table S1 (10–12, 15–17). Besides ASP5, which localizes to the Golgi (15–17), these proteins all localize to the PV/PVM.

The newly identified components described here do not display any homology to known protein translocation machinery based on BLAST analysis results (BLASTP 2.10.0+), making it difficult to infer their functions and thus which, if any, are part of an actual translocon remains unknown. In addition to lacking homology to known translocation machinery, MYR4 and GRA45 do not have detectable homology to any other known, functional protein domains and neither do they share homology to proteins in any species outside of *Coccidia/Eimeriorina*. Like MYR1, MYR2, MYR3, and ROP17, however, MYR4, GRA44 and GRA45 all have clear orthologs in *Hammondia hammondi* and *Neospora caninum* (**Table S1**).

GRA44, by contrast, contains a putative phosphatase domain that shares homology to a region of the *Plasmodium* serine/threonine phosphatase UIS2 (28% identity over 21% of the protein; BLASTP 2.10.0+), which has recently been shown to localize to the *Plasmodium* PVM in liver stage parasites (40). Whether UIS2 plays a role in protein translocation in *Plasmodium* remains to be determined but this would be

surprising given that none of the other components of the complex known to promote translocation in *Plasmodium* (known as PTEX) so far studied play a role in translocation in *Toxoplasma* (2). Additionally, whether this phosphatase domain is important for effector export in *Toxoplasma* is not yet known. Given that the kinase domain of ROP17 is necessary for GRA16 export (12) it is intriguing that two of the eight factors necessary for effector export are either a kinase or a phosphatase. There are numerous serine residues that are phosphorylated among MYR1, MYR2, MYR3, and MYR4, supporting the possibility that phosphorylation of the translocation machinery is critical to regulating its function in effector export. While this work was in progress, we learned of similar studies by Blakely, Arrizabalaga and colleagues who also found that GRA44 associates with MYR1 and is necessary for efficient c-Myc upregulation during infection (see accompanying manuscript). These latter authors used a knockdown approach to study GRA44 and saw a more dramatic impact of GRA44 loss on parasite growth than we report here for the GRA44 knockout; this might indicate that compensatory changes were selected for during the prolonged selection necessary to generate and expand our knockout clone, as was reported for AMA1 knockouts that showed dramatic up-regulation of the paralogue, AMA2 (41). Thus, transcriptomic analysis of the GRA44 knockout may reveal clues to its specific role(s) in *Toxoplasma* tachyzoites.

Our results expand the enigmas of why some parasite proteins are proteolytically processed by ASP5, and why ASP5 is essential for effector translocation across the PVM. MYR1, GRA44, and GRA45 all possess “RRL” motifs that appear to be cleaved in an ASP5-dependent manner yet, surprisingly, their function in the export of GRA16, and of GRA24 in the case of MYR1 (24), appears agnostic to mutation of these sites.

For MYR1, we previously showed that the two domains generated by ASP5 processing stay connected through a disulfide bond after cleavage (11); it remains to be determined whether the polypeptides formed by RRL cleavage in GRA44 and GRA45 likewise associate in a similar manner. It is also important to note that our assays may not be sensitive enough to detect small changes in protein abundance in the host nucleus, and that it is the combination of multiple proteins not being processed by ASP5 that is deleterious to export in *Δasp5* mutants, rather than the result of failure to cleave any single protein.

Interestingly, there was a large number of proteins that were more highly enriched than MYR3 in our immunoprecipitations with MYR1, and it remains a strong possibility that additional MYR1-associating proteins are involved in effector translocation. Due to the large number of enriched proteins and the limited throughput of our approach, we were unable to investigate all candidates for such a role; nevertheless, our data showing that GRA16-HA export is not lost in parasites disrupted for *GRA7*, *CST1*, *MAF1*, *PPM3C*, or *GRA54* strongly suggests that it is not general PV/PVM disruption that results in the loss of effector translocation. Further work will be needed to determine which of the remaining proteins we see enriched in the MYR1 immunoprecipitations are there because of specific association with MYR1 vs. nonspecific associations of proteins within the PV/PVM due to association within lipid rafts or other entities.

Lastly, none of *GRA44*, *GRA45*, or *MYR4* were identified in the forward genetic screen of parasites that are unable to induce c-Myc (10). This could be due to the growth defects observed in Δ*myr4,* Δ*gra44,* and Δ*gra45* parasites shown here since

parasites with null mutations in these genes might be lost during the 7-8 rounds of selection used in that screen due to a fitness disadvantage. Alternatively, the mutagenesis-based genetic screen was not saturating and so a more comprehensive, genome-wide screen using CRISPR/Cas9 technologies might reveal these and other genes responsible for effector translocation in *Toxoplasma*. Regardless, our finding of three new components of the export machinery provides a richer understanding of how *Toxoplasma* delivers effectors into host cells. Future work will determine the precise function of each, including how they interact, the role of ASP5 cleavage, and which, if any, constitutes the actual translocon.

Materials and Methods

Parasite strains, culture and infections

All *Toxoplasma* tachyzoites used in this study are in the Type I "RH" background, either RH::*MYR1-3xHA* (11), RHΔ*gra16::GRA16HA* (6), RHΔ*maf1* (31), RHΔ*hpt* (42), or RHΔ*hpt*Δ*ku80* (43). These tachyzoites, and all subsequently generated lines, were propagated in human foreskin fibroblasts (HFFs) cultured in complete Dulbecco's Modified Eagle Medium (cDMEM) supplemented with 10% heat-inactivated fetal bovine serum (FBS; HyClone, Logan, UT), 2 mM L-glutamine, 100 U/ml penicillin and 100 µg/ml streptomycin at 37 °C with 5% CO_2. The HFFs were obtained from the neonatal clinic at Stanford University following routine circumcisions that are performed at the request of the parents for cultural, health or other personal medical reasons (i.e., not in any way related to research). These foreskins, which would otherwise be discarded, are fully de-identified and therefore do not constitute "human subjects research".

Prior to infection, parasites were scraped and syringe-lysed using a 27 G needle, counted using a hemocytometer, and added to HFFs. "Mock" infection was done by first syringe-lysing uninfected HFFs, processing this in the same manner as done for the infected cells, and then adding the same volume of the resulting material as used for infections. For experiments where human c-Myc protein was detected, the parasites were added to HFFs in media containing 0% serum.

Immunofluorescence assay (IFA)

Infected cells grown on glass coverslips were fixed and permeabilized using 100% cold methanol for 10 min. Samples were washed 3x with PBS and blocked using

3% BSA in PBS for 1 hour at room temperature (RT). HA was detected with rat monoclonal anti-HA antibody 3F10 (Roche), SAG1 was detected with mouse anti-SAG1 monoclonal antibody DG52 (44), GRA7 was detected with rabbit anti-GRA7 antibodies (45), V5 was detected with mouse anti-V5 tag monoclonal antibody (Invitrogen), and c-Myc was detected with rabbit monoclonal anti-c-Myc antibody Y69 (Abcam). Primary antibodies were detected with goat polyclonal Alexa Fluor-conjugated secondary antibodies (Invitrogen). Primary and secondary antibodies were both diluted in 3% BSA in PBS. Coverslips were incubated with primary antibodies for 1 hour at RT, washed, and incubated with secondary antibodies for 1 hour at RT. Vectashield with DAPI stain (Vector Laboratories) was used to mount the coverslips on slides. Fluorescence was detected using wide-field epifluorescence microscopy and images were analyzed using ImageJ. All images shown for any given condition/staining in any given comparison/dataset were obtained using identical parameters.

Transfections

All transfections were performed using the Amaxa 4D Nucleofector (Lonza) model. Tachyzoites were mechanically released in PBS, pelleted, and resuspended in 20 µL P3 Primary Cell Nucleofector Solution (Lonza) with 5-25 µg DNA for transfection. After transfection, parasites were allowed to infect HFFs in DMEM.

Plasmid construction

For gene disruption plasmids: gRNAs designed against a PAM site of each gene of interest were cloned into the pU6-Universal plasmid. pU6-Universal was a gift from Sebastian Lourido (Addgene plasmid # 52694 ; http://n2t.net/addgene:52694 ; RRID:Addgene_52694).

For ectopic expression plasmids: The pGRA-V5 plasmid was created by replacing the HA tag sequence in the pGRA-HPT-HA plasmid (46) with the V5 tag DNA sequence (GGCAAGCCCATCCCCAACCCCCTGCTGGGCCTGGACAGCAC) and removing the HPT resistance cassette using standard molecular biology techniques. The pX-V5 plasmid was created by removing the GRA1 promoter from pGRA-V5 using standard molecular biology techniques. Complementation plasmids to ectopically express V5 tagged proteins off their native promoters were created by PCR amplification of the open reading frame of each gene, minus the stop codon, plus ~2000 bp upstream of the start codon to include the native promoter, followed by cloning into pX-V5 using Gibson Assembly (NEB). RRL→ARL or RRL→AAA mutated complementation plasmids were generated using overlap extension PCR using primers harboring the mutation and cloning the resultant products into pX-V5 using Gibson Assembly (NEB).

For endogenous tagging plasmids: Approximately 1500-3000 bp of the 3' coding sequence of each gene was amplified from RH genomic DNA and cloned into the pTKO2-HPT-3xHA plasmid (11) using either Gibson Assembly (NEB) or by cloning into the EcoRV and NotI restriction sites.

A list of all primers and plasmids used and generated in this study can be found in **File S2**.

Endogenous tagging

Endogenous tagging plasmids were transfected into *Toxoplasma* via electroporation. Tachyzoites were allowed to infect HFFs in T25 flasks for 24 hours, after which the medium was changed to complete DMEM supplemented with 50 µg/ml

464 mycophenolic acid and 50 µg/ml xanthine for selection for the hypoxanthine-xanthine-
465 guanine-phosphoribosyltransferae (HXGPRT or HPT) marker for 3-5 days.

466 **Gene disruption**

467 A list of all sgRNA sequences used in this study can be found in **File S2**.
468 RHΔ*gra16*::GRA16HA tachyzoites were transfected with pTKO2-CAT-mCherry (CAT is
469 chloramphenicol acetyl transferase which confers resistance to chloramphenicol; the
470 plasmid was a gift from Ian Foe and Matthew Bogyo (47)) and the corresponding
471 modified pU6-sgRNA plasmid and allowed to infect HFFs for 24-48 hours. For gene
472 disruption of MYR3, the previously published pSAG1:U6-Cas9:sgMYR3 plasmid was
473 used instead (11). Between 24-48 hours after transfection, DMEM media with 80 µM
474 chloramphenicol was added to the cells. The media was replaced with fresh
475 chloramphenicol-supplemented media every 48-72 hours. After at least 7 days in
476 selection, single clones were selected from the transfected populations in 96 well plates
477 using limiting dilution. Single clones were maintained in chloramphenicol-supplemented
478 media until confirmation of the genetic disruption.

479 **Ectopic expression**

480 Plasmids for ectopic expression were transiently transfected into *Toxoplasma*
481 using electroporation. Tachyzoites were allowed to infect HFFs for 18-24 hours before
482 assessing for expression of the ectopically expressed protein via either IFA or western
483 blotting.

484 **Western blotting**

485 Cell lysates were prepared at the indicated time points post-infection in Laemmli
486 sample buffer (BioRad). The samples were boiled for 5 min, separated by SDS-PAGE,

and transferred to polyvinylidene difluoride (PVDF) membranes. Membranes were blocked with 5% nonfat dry milk in TBS supplemented with 0.5% Tween-20, and proteins were detected by incubation with primary antibodies diluted in blocking buffer followed by incubation with secondary antibodies (raised in goat against the appropriate species) conjugated to horseradish peroxidase (HRP) and diluted in blocking buffer. HA was detected using a horseradish peroxidase (HRP)-conjugated HA antibody (Roche cat no. 12013819001), SAG2A was detected using rabbit polyclonal anti-SAG2A antibodies (48), Cyclin E1 was detected using mouse monoclonal antibody HE12 (Santa Cruz Biotechnology), and GAPDH was detected using mouse monoclonal anti-GAPDH antibody 6C5 (Calbiochem). Horseradish peroxidase (HRP) was detected using enhanced chemiluminescence (ECL) kit (Pierce).

Plaque assay

Parasites were syringe-released from HFFs and added to confluent HFFs in T25 flasks. After 7 days, the infected monolayers were washed with PBS, fixed with methanol, and stained with crystal violet. Plaque area was measured using ImageJ.

Immunoprecipitations (IPs) for mass spectrometry

IPs to identify MYR1-interacting proteins in HFFs were performed as follows. One 15-cm dish of HFFs for each infection condition was grown to confluence. HFFs were infected with either 15 x 10^6 RH::*MYR1-3xHA* or RHΔ*hpt* parasites for 24 hours. Infected cells were washed 3 times in cold PBS and then scraped into 1 mL cold cell lysis buffer (50mM Tris (pH 8.0), 150mM NaCl, 0.1% (v/v) Nonidet P-40 Alternative [CAS no. 9016-45-9]) supplemented with complete protease inhibitor cocktail (cOmplete, EDTA-free [Roche]). Cell lysates were passed 3 times through a 25 G

needle, followed by 3 times through a 27 G needle, followed by sonication on ice (Branson Sonifier 250), with 3 pulses of 10 s at 50% duty cycle and output control 2. Cell lysates were spun at 1000 × *g* for 10 min to remove insoluble material and unlysed cells. Lysates were added to 100 µL magnetic beads conjugated to anti-HA antibodies (Pierce) and incubated overnight rotating at 4 °C. Unbound protein lysate was removed, and the anti-HA magnetic beads were then washed 10 times in cell lysis buffer. HA-tagged MYR1, and associated proteins, were eluted in 60 µL pH 2.0 buffer (Pierce) for 10 min at 50 °C to dissociate proteins from the antibody-conjugated beads. The elutions were immediately neutralized 1:10 with pH 8.5 neutralization buffer (Pierce).

Mass spectrometry sample preparation

45 µL of each IP elution was combined with 15 µL of 4X Laemmli sample buffer supplemented with BME (BioRad), boiled for 10 min at 95 °C, and loaded on a Bolt 4-12% Bis-Tris gel (Invitrogen). The samples were resolved for approximately 8 min at 150V. The gel was washed once in UltraPure water (Thermo), fixed in 50% methanol and 7% acetic acid for 15 min, followed by 3 additional washes with UltraPure water. The gel was stained for 10 min with GelCode Blue (Thermo) and washed with UltraPure water for an additional 20 min. One gel band (approx. 1.5 cm in size) for each condition was excised and de-stained for 2 hours in a 50% methanol and 10% acetic acid solution, followed by a 30 min soak in UltraPure water. Each gel slice was cut into 1 mm x 1 mm squares, covered in 1% acetic acid solution, and stored at 4 °C until the in-gel digestion could be performed.

To prepare samples for mass spectrometry, the 1% acetic acid solution was removed, 10 µl of 50 mM DTT was added, and volume was increased to 100 µl with 50

mM ammonium bicarbonate. Samples were incubated at 55 °C for 30 min. Samples were then brought down to RT, DTT solution was removed, 10 µl of 100 mM acrylamide (propionamide) was added and volume was again normalized to 100 µl with 50 mM ammonium bicarbonate followed by an incubation at RT for 30 min. Acrylamide solution was removed, 10 µl (0.125 µg) of Trypsin/LysC (Promega) solution was added and another 50 µl of 50 mM ammonium bicarbonate was added to cover the gel pieces. Samples were incubated overnight at 37 °C for peptide digestion. Solution consisting of digested peptides was collected in fresh Eppendorf tubes, 50 µl of extraction buffer (70% acetonitrile, 29% water, 1% formic acid) was added to gel pieces, incubated at 37 °C for 10 min, centrifuged at 10,000 x g for 2 minutes and collected in the same tubes consisting of previous elute. This extraction was repeated one more time. Collected extracted peptides were dried to completion in a speed vac and stored at 4 °C until ready for mass spectrometry.

Mass spectrometry

Eluted, dried peptides were dissolved in 12.5 µl of 2% acetonitrile and 0.1% formic acid and 3 µl was injected into an in-house packed C18 reversed phase analytical column (15 cm in length). Peptides were separated using a Waters M-Class UPLC, operated at 450 nL/min using a linear 80 minute gradient from 4-40% mobile phase B. Mobile phase A consisted of 0.2% formic acid, 99.8% water, Mobile phase B was 0.2% formic acid, 99.8% acetonitrile. Ions were detected using an Orbitrap Fusion mass spectrometer operating in a data dependent fashion using typical “top speed” methodologies. Ions were selected for fragmentation based on the most intense multiply

555 charged precursor ions using Collision induced dissociation (CID). Data from these
556 analyses was then transferred for analysis.

557 **Mass spectrometric analysis**

558 The .RAW data were searched using MaxQuant version 1.6.1.0 against the
559 canonical human database from UniProt, *Toxoplasma* GT1 databases from ToxoDB
560 (versions 7.3 and 37.0), and the built-in contaminant database. Specific parameters
561 used in the MaxQuant analysis can be found in **File S1**. Peptide and protein
562 identifications were filtered to a 1% false discovery rate (FDR) and reversed proteins,
563 contaminants, and proteins only identified by a single modification site, were removed
564 from the dataset. MYR1-3xHA enrichment over the non-HA tagged RH was determined
565 by adding 1 to each spectral count (tandem MS [MS/MS count]) and calculating the
566 NSAF (number of spectral counts identifying a protein divided by the protein's length,
567 divided by the sum of all spectral counts/lengths for all proteins in the experiment). The
568 average MYR1-3xHA enrichment from the two biological replicates (IP 1 and IP 2) was
569 used to determine the protein ranking.

570 **Data availability**

571 The mass spectrometry proteomics data have been deposited to the
572 ProteomeXchange Consortium (http://proteomecentral.proteomexchange.org) via the
573 PRIDE partner repository (49) with the dataset identifier PXD016383.

574

Acknowledgements

We thank all members of our laboratory, as well as Melanie Espiritu for help with tissue culture and ordering, Ian Foe and Matthew Bogyo for providing reagents, Ryan Leib and Kratika Singhal for helpful advice regarding mass spectrometry, and Will Blakely and Gustavo Arrizabalaga for helpful discussions and exchange of data prior to publication. Special thanks to the Vincent Coates Foundation Mass Spectrometry Laboratory at Stanford University Mass Spectrometry (SUMS) for assistance in processing mass spectrometry samples.

This project has been funded in whole or part with federal funds from the U.S. National Institute of Allergy and Infectious Diseases, National Institutes of Health, Department of Health and Human Services, under awards NIH RO1-AI021423 (J.C.B.) and NIH RO1-AI129529 (J.C.B.), NIH T32-AI732832 (A.M.C.), NIH T32-AI007328 (T.C.T.), NIH T32-AI732832 (A.G.M.), NIH F31-AI120649 (N.D.M.), with funds from the National Science Foundation Graduate Research Fellowship Program (https://www.nsfgrfp.org/) under grant DGE-114747 (A.M.C.), with support from the Stanford Bio-X Graduate Research Fellowship (T.C.T.), and with grant NIH P30 CA124435 for utilization of the Stanford Cancer Institute Proteomics/Mass Spectrometry Shared Resource. The funders had no role in study design, data collection and analysis, decision to publish, or preparation of the manuscript.

References

1. Hill DE, Chirukandoth S, Dubey JP. 2005. Biology and epidemiology of Toxoplasma gondii in man and animals . Anim Heal Res Rev.

2. Rastogi S, Cygan AM, Boothroyd JC. 2019. Translocation of effector proteins into host cells by Toxoplasma gondii. Curr Opin Microbiol.

3. Bougdour A, Durandau E, Brenier-Pinchart MP, Ortet P, Barakat M, Kieffer S, Curt-Varesano A, Curt-Bertini RL, Bastien O, Coute Y, Pelloux H, Hakimi MA. 2013. Host cell subversion by Toxoplasma GRA16, an exported dense granule protein that targets the host cell nucleus and alters gene expression. Cell Host Microbe2013/04/23. 13:489–500.

4. Braun L, Brenier-Pinchart MP, Yogavel M, Curt-Varesano A, Curt-Bertini RL, Hussain T, Kieffer-Jaquinod S, Coute Y, Pelloux H, Tardieux I, Sharma A, Belrhali H, Bougdour A, Hakimi MA. 2013. A Toxoplasma dense granule protein, GRA24, modulates the early immune response to infection by promoting a direct and sustained host p38 MAPK activation. J Exp Med 210:2071–2086.

5. Gay G, Braun L, Brenier-Pinchart MP, Vollaire J, Josserand V, Bertini RL, Varesano A, Touquet B, De Bock PJ, Coute Y, Tardieux I, Bougdour A, Hakimi MA. 2016. Toxoplasma gondii TgIST co-opts host chromatin repressors dampening STAT1-dependent gene regulation and IFN-gamma-mediated host defenses. J Exp Med 213:1779–1798.

6. Panas MW, Naor A, Cygan AM, Boothroyd JC. 2019. Toxoplasma Controls Host Cyclin E Expression through the Use of a Novel MYR1-Dependent Effector Protein, HCE1. MBio2019/05/02. 10.

7. Nadipuram SM, Kim EW, Vashisht AA, Lin AH, Bell HN, Coppens I, Wohlschlegel JA, Bradley PJ. 2016. In Vivo biotinylation of the toxoplasma parasitophorous vacuole reveals novel dense granule proteins important for parasite growth and pathogenesis. MBio 7.

8. He H, Brenier-Pinchart MP, Braun L, Kraut A, Touquet B, Coute Y, Tardieux I, Hakimi MA, Bougdour A. 2018. Characterization of a Toxoplasma effector uncovers an alternative GSK3/beta-catenin-regulatory pathway of inflammation. Elife 7.

9. Braun L, Brenier-Pinchart MP, Hammoudi PM, Cannella D, Kieffer-Jaquinod S, Vollaire J, Josserand V, Touquet B, Couté Y, Tardieux I, Bougdour A, Hakimi MA. 2019. The Toxoplasma effector TEEGR promotes parasite persistence by modulating NF-κB signalling via EZH2. Nat Microbiol.

10. Franco M, Panas MW, Marino ND, Lee MCW, Buchholz KR, Kelly FD, Bednarski JJ, Sleckman BP, Pourmand N, Boothroyd JC. 2016. A novel secreted protein, MYR1, is central to Toxoplasma's manipulation of host cells. MBio 7.

11. Marino ND, Panas MW, Franco M, Theisen TC, Naor A, Rastogi S, Buchholz KR, Lorenzi HA, Boothroyd JC. 2018. Identification of a novel protein complex essential for effector translocation across the parasitophorous vacuole membrane of Toxoplasma gondii. PLoS Pathog 14:e1006828.

12. Panas MW, Ferrel A, Naor A, Tenborg E, Lorenzi HA, Boothroyd JC. 2019. Translocation of Dense Granule Effectors across the Parasitophorous Vacuole Membrane in Toxoplasma- Infected Cells Requires the Activity of ROP17, a Rhoptry Protein Kinase . mSphere.

642 13. El Hajj H, Lebrun M, Arold ST, Vial H, Labesse G, Dubremetz JF. 2007. ROP18 Is
643 a Rhoptry Kinase Controlling the Intracellular Proliferation of Toxoplasma gondii.
644 PLoS Pathog 3:e14.
645 14. Etheridge RD, Alaganan A, Tang K, Lou HJ, Turk BE, Sibley LD. 2014. The
646 Toxoplasma pseudokinase ROP5 forms complexes with ROP18 and ROP17
647 kinases that synergize to control acute virulence in mice. Cell Host Microbe
648 15:537–550.
649 15. Coffey MJ, Sleebs BE, Uboldi AD, Garnham A, Franco M, Marino ND, Panas MW,
650 Ferguson DJ, Enciso M, O'Neill MT, Lopaticki S, Stewart RJ, Dewson G, Smyth
651 GK, Smith BJ, Masters SL, Boothroyd JC, Boddey JA, Tonkin CJ. 2015. An
652 aspartyl protease defines a novel pathway for export of Toxoplasma proteins into
653 the host cell. Elife 4.
654 16. Hammoudi PM, Jacot D, Mueller C, Di Cristina M, Dogga SK, Marq JB, Romano
655 J, Tosetti N, Dubrot J, Emre Y, Lunghi M, Coppens I, Yamamoto M, Sojka D, Pino
656 P, Soldati-Favre D. 2015. Fundamental Roles of the Golgi-Associated
657 Toxoplasma Aspartyl Protease, ASP5, at the Host-Parasite Interface. PLoS
658 Pathog 11:e1005211.
659 17. Curt-Varesano A, Braun L, Ranquet C, Hakimi MA, Bougdour A. 2016. The
660 aspartyl protease TgASP5 mediates the export of the Toxoplasma GRA16 and
661 GRA24 effectors into host cells. Cell Microbiol 18:151–167.
662 18. Russo I, Babbitt S, Muralidharan V, Butler T, Oksman A, Goldberg DE. 2010.
663 Plasmepsin v licenses Plasmodium proteins for export into the host erythrocyte.
664 Nature.

19. Boddey JA, Hodder AN, Günther S, Gilson PR, Patsiouras H, Kapp EA, Pearce JA, De Koning-Ward TF, Simpson RJ, Crabb BS, Cowman AF. 2010. An aspartyl protease directs malaria effector proteins to the host cell. Nature.

20. Hiller NL, Bhattacharjee S, van Ooij C, Liolios K, Harrison T, Lopez-Estrano C, Haldar K. 2004. A host-targeting signal in virulence proteins reveals a secretome in malarial infection. Science (80-) 306:1934–1937.

21. Marti M, Good RT, Rug M, Knuepfer E, Cowman AF. 2004. Targeting malaria virulence and remodeling proteins to the host erythrocyte. Science (80-) 306:1930–1933.

22. Heiber A, Kruse F, Pick C, Gruring C, Flemming S, Oberli A, Schoeler H, Retzlaff S, Mesen-Ramirez P, Hiss JA, Kadekoppala M, Hecht L, Holder AA, Gilberger TW, Spielmann T. 2013. Identification of new PNEPs indicates a substantial non-PEXEL exportome and underpins common features in Plasmodium falciparum protein export. PLoS Pathog 9:e1003546.

23. Spielmann T, Hawthorne PL, Dixon MW, Hannemann M, Klotz K, Kemp DJ, Klonis N, Tilley L, Trenholme KR, Gardiner DL. 2006. A cluster of ring stage-specific genes linked to a locus implicated in cytoadherence in Plasmodium falciparum codes for PEXEL-negative and PEXEL-positive proteins exported into the host cell. Mol Biol Cell2006/06/09. 17:3613–3624.

24. Naor A, Panas MW, Marino N, Coffey MJ, Tonkin CJ, Boothroyd JC. 2018. MYR1-Dependent Effectors Are the Major Drivers of a Host Cell's Early Response to Toxoplasma, Including Counteracting MYR1-Independent Effects. MBio 9.

25. Florens L, Carozza MJ, Swanson SK, Fournier M, Coleman MK, Workman JL,

688 Washburn MP. 2006. Analyzing chromatin remodeling complexes using shotgun
689 proteomics and normalized spectral abundance factors. Methods 40:303–311.
690 26. de Koning-Ward TF, Gilson PR, Boddey JA, Rug M, Smith BJ, Papenfuss AT,
691 Sanders PR, Lundie RJ, Maier AG, Cowman AF, Crabb BS. 2009. A newly
692 discovered protein export machine in malaria parasites. Nature 459:945–949.
693 27. Coffey MJ, Dagley LF, Seizova S, Kapp EA, Infusini G, Roos DS, Boddey JA,
694 Webb AI, Tonkin CJ. 2018. Aspartyl Protease 5 Matures Dense Granule Proteins
695 That Reside at the Host-Parasite Interface in Toxoplasma gondii. MBio.
696 28. Zhang YW, Halonen SK, Ma YF, Wittner M, Weiss LM. 2001. Initial
697 characterization of CST1, a Toxoplasma gondii cyst wall glycoprotein. Infect
698 Immun 69:501–507.
699 29. Fischer HG, Stachelhaus S, Sahm M, Meyer HE, Reichmann G. 1998. GRA7, an
700 excretory 29 kDa Toxoplasma gondii dense granule antigen released by infected
701 host cells. Mol Biochem Parasitol 91:251–262.
702 30. Tu V, Mayoral J, Sugi T, Tomita T, Han B, Ma YF, Weissa LM. 2019. Enrichment
703 and proteomic characterization of the cyst wall from in vitro toxoplasma gondii
704 cysts. MBio.
705 31. Pernas L, Adomako-Ankomah Y, Shastri AJ, Ewald SE, Treeck M, Boyle JP,
706 Boothroyd JC. 2014. Toxoplasma Effector MAF1 Mediates Recruitment of Host
707 Mitochondria and Impacts the Host Response. PLoS Biol 12.
708 32. Huynh MH, Carruthers VB. 2009. Tagging of endogenous genes in a Toxoplasma
709 gondii strain lacking Ku80. Eukaryot Cell2009/02/17. 8:530–539.
710 33. Shirai A, Matsuyama A, Yashiroda Y, Hashimoto A, Kawamura Y, Arai R,

711 Komatsu Y, Horinouchi S, Yoshida M. 2008. Global analysis of gel mobility of
712 proteins and its use in target identification. J Biol Chem.
713 34. Treeck M, Sanders JL, Elias JE, Boothroyd JC. 2011. The Phosphoproteomes of
714 Plasmodium falciparum and Toxoplasma gondii Reveal Unusual Adaptations
715 Within and Beyond the Parasites' Boundaries. Cell Host Microbe2011/10/25.
716 10:410–419.
717 35. Sidik SM, Huet D, Ganesan SM, Huynh MH, Wang T, Nasamu AS, Thiru P, Saeij
718 JP, Carruthers VB, Niles JC, Lourido S. 2016. A Genome-wide CRISPR Screen in
719 Toxoplasma Identifies Essential Apicomplexan Genes. Cell 166:1423-1435 e12.
720 36. Adomako-Ankomah Y, English ED, Danielson JJ, Pernas LF, Parker ML,
721 Boulanger MJ, Dubey JP, Boyle JP. 2016. Host Mitochondrial Association
722 Evolved in the Human Parasite Toxoplasma gondii via Neofunctionalization of a
723 Gene Duplicate. Genetics.
724 37. Franco M, Shastri AJ, Boothroyd JC. 2014. Infection by Toxoplasma gondii
725 Specifically Induces Host c-Myc and the Genes This Pivotal Transcription Factor
726 Regulates. Eukaryot Cell 13:483–493.
727 38. Russo I, Babbitt S, Muralidharan V, Butler T, Oksman A, Goldberg DE. 2010.
728 Plasmepsin V licenses Plasmodium proteins for export into the host erythrocyte.
729 Nature 463:632–636.
730 39. Boddey JA, Hodder AN, Gunther S, Gilson PR, Patsiouras H, Kapp EA, Pearce
731 JA, de Koning-Ward TF, Simpson RJ, Crabb BS, Cowman AF. 2010. An aspartyl
732 protease directs malaria effector proteins to the host cell. Nature 463:627–631.
733 40. Schnider CB, Bausch-Fluck D, Brühlmann F, Heussler VT, Burda P-C. 2018.

734 BioID Reveals Novel Proteins of the Plasmodium Parasitophorous Vacuole
735 Membrane. mSphere.
736 41. Lamarque MH, Roques M, Kong-Hap M, Tonkin ML, Rugarabamu G, Marq JB,
737 Penarete-Vargas DM, Boulanger MJ, Soldati-Favre D, Lebrun M. 2014. Plasticity
738 and redundancy among AMA-RON pairs ensure host cell entry of Toxoplasma
739 parasites. Nat Commun 5:4098.
740 42. Donald RGK, Carter D, Ullman B, Roos DS. 1996. Insertional tagging, cloning,
741 and expression of the Toxoplasma gondii hypoxanthine-xanthine-guanine-
742 phosphoribosyltransferase gene. J Biol Chem 271:14010–14019.
743 43. Fox BA, Ristuccia JG, Gigley JP, Bzik DJ. 2009. Efficient gene replacements in
744 Toxoplasma gondii strains deficient for nonhomologous end joining. Eukaryot
745 Cell2009/02/17. 8:520–529.
746 44. Burg JL, Perelman D, Kasper LH, Ware PL, Boothroyd JC. 1988. Molecular
747 analysis of the gene encoding the major surface antigen of Toxoplasma gondii. J
748 Immunol 141:3584–3591.
749 45. Dunn JD, Ravindran S, Kim SK, Boothroyd JC. 2008. The Toxoplasma gondii
750 dense granule protein GRA7 is phosphorylated upon invasion and forms an
751 unexpected association with the rhoptry proteins ROP2 and ROP4. Infect Immun
752 76:5853–5861.
753 46. Saeij JPJ, Boyle JP, Coller S, Taylor S, Sibley LD, Brooke-Powell ET, Ajioka JW,
754 Boothroyd JC. 2006. Polymorphic Secreted Kinases Are Key Virulence Factors in
755 Toxoplasmosis. Science (80-) 314:1780–1783.
756 47. Foe IT, Onguka O, Amberg-Johnson K, Garner RM, Amara N, Beatty W, Yeh E,

Bogyo M. 2018. The Toxoplasma gondii Active Serine Hydrolase 4 Regulates Parasite Division and Intravacuolar Parasite Architecture. mSphere 3.

48. Grigg ME, Bonnefoy S, Hehl AB, Suzuki Y, Boothroyd JC. 2001. Success and virulence in Toxoplasma as the result of sexual recombination between two distinct ancestries. Science (80-) 294:161–165.

49. Vizcaíno JA, Csordas A, Del-Toro N, Dianes JA, Griss J, Lavidas I, Mayer G, Perez-Riverol Y, Reisinger F, Ternent T, Xu QW, Wang R, Hermjakob H. 2016. 2016 update of the PRIDE database and its related tools. Nucleic Acids Res.

Figures and Figure Legends

Supplemental File 1.

Mass spectrometry analysis parameters and results for proteins that coimmunoprecipitate with MYR1-3xHA-expressing and untagged RH parasites. For all sheets, the IDs corresponding to the majority proteins, i.e., the proteins which contained at least half of the peptides belonging to a protein group (grouping of proteins which cannot be unambiguously identified by unique peptides), the number of spectral counts (MS/MS count), the average NSAF enrichment score (MYR1/RH Enrichment, as further elaborated in Materials and Methods), and the protein rank as defined by the enrichment score corresponding to each grouping are shown. The gene product (for *Toxoplasma* proteins) or associated gene name (for human proteins) for the first listed protein ID in each row is shown in the Description column. Sheet 1 ("Toxo_proteins") shows the experimental data sets for *Toxoplasma* proteins only, listed in rank order by the average NSAF enrichment from both experiments. Sheet 2 ("All_proteins") shows the experimental data sets for both human and *Toxoplasma* proteins, listed in rank order by the average NSAF enrichment from both experiments. Sheet 3 ("Parameters") shows the parameters used in the MaxQuant analysis.

Supplemental File 2.

Primers, sgRNA sequences, and plasmids used and/or generated in this study.

Supplemental Table 1.

Summary of *Toxoplasma* genes necessary for effector translocation. The number of predicted transmembrane domains, number of "RRL" motifs, and CRISPR phenotype score are listed for each *Toxoplasma* gene necessary for effector translocation identified thus far. Additionally, the percent identities of each of these genes to their orthologs in *Hammondia hammondi* and *Neospora caninum*, and whether the "RRL" sequences are conserved in these species are also listed. Transmembrane domain prediction based on Phobius (Lukas Kall et al., Nucleic Acids Res 35:W429-32, 2007, https://doi.org/10.1093/nar/gkm256). CRISPR phenotype scores are from Sidik et al. (Cell 166(6):1423-1435.e12, https:// 10.1016/j.cell.2016.08.019). Identity calculated by comparison to head-to-head comparison of ortholog in indicated species using Sequence Manipulation Suite (Stothard P, Biotechniques 28:1102-1104, https://doi.org/ 10.2144/00286ir01).

Supplemental Figure 1.

A. Western blot of endogenously tagged 211460-3xHA single clone and population. HFFs were infected with RHΔ*hpt*Δ*ku80* tachyzoites (RH) or endogenously tagged RH::*211460-3xHA* parasites (either from the population or an independently generated single clone). Lysates from infected HFFs were prepared and 211460-3xHA was detected by western blotting using rat anti-HA antibodies. Rabbit anti-SAG2A staining was used as a loading control for total parasite protein. The western blot for the 211460-3xHA population is the same data as presented in Fig 2A. Approximate migration of a ladder of size standards (sizes in kDa) is indicated.

B. Immunofluorescence microscopy of endogenously tagged 211460-3xHA from an independently generated single clone. Tachyzoites were allowed to infect HFFs for 16 hours before the infected monolayer was fixed with methanol. 211460-3xHA was detected with rat anti-HA antibodies, *Toxoplasma* tachyzoites were detected with mouse anti-SAG1 antibodies, and the infected monolayer was visualized with DIC. Scale bar is 10μm.

Supplemental Figure 2.

Immunofluorescence microscopy of endogenously tagged proteins in extracellular parasites. The populations of endogenously tagged parasites analyzed in Fig. 2A were seeded onto empty coverslips before being fixed with methanol. The corresponding tagged proteins were detected with rat anti-HA antibodies, the marker for dense granule proteins, GRA7, was detected with rabbit anti-GRA7 antibodies, and the parasites were visualized with differential interference microscopy (DIC). Scale bar is 5μm.

Supplemental Figure 3.

A. Schematic of CRISPR-mediated gene disruption of candidate genes. Primers flanking the guide-targeted region, indicated by “Forward” and “Reverse”, were constructed to amplify a ~1000bp region of the native, uninterrupted gene. pTKO2-CAT-mCherry is the plasmid used for integration and selection.

B. PCR amplifications of genomic DNA from RHΔ*gra16*::GRA16-HA parasites (parental) and from a chloramphenicol-resistant (CAT^+) clonal strain with disruption of the indicated gene using the forward and reverse primers shown in Panel A. Sizes (base pairs) of the standard ladder are shown. Bands of the

837 expected size in the parental strain (~1000bp) and either lack of a band or
838 presence of altered bands in the disrupted strains, indicate insertion of the
839 selection plasmid within the targeted gene, as indicated (e.g., Δ*myr3* is a strain
840 with a disruption of the *MYR3* locus).
841
842 **Supplemental Figure 4.**
843 Immunofluorescence microscopy of GRA16-HA nuclear localization and human nuclear
844 c-Myc expression in HFFs infected with the indicated disrupted parasite strains.
845 Tachyzoites were allowed to infect HFFs (without serum) for 18 hours before the
846 infected monolayers were fixed with methanol and stained with rat anti-HA antibodies
847 and rabbit anti-c-Myc antibodies. Host nuclei were visualized using DAPI. Scale bar is
848 20μm.
849
850 **Supplemental Figure 5.**
851 Western blot of human cyclin E1 protein in cells infected with the indicated parasite
852 strain. HFFs were infected with the indicated strain of tachyzoites, or mock-treated with
853 uninfected HFF lysate, for 20 hours before lysates were generated for immunoblotting.
854 Lysates were analyzed by western blotting using mouse anti-cyclin E1 antibodies.
855 Rabbit anti-SAG2A was used to assess the levels of parasite protein in the lysate.
856

A

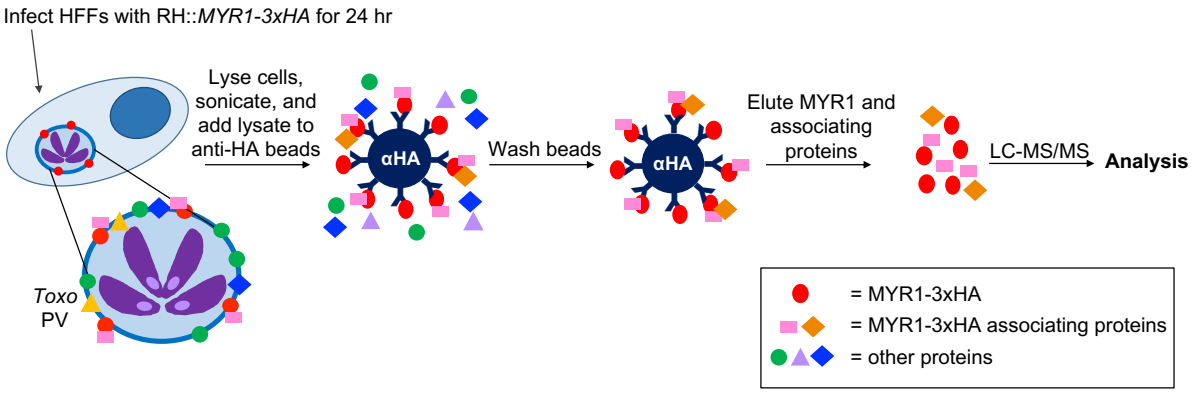

B

		MS/MS Count					
		MYR1		RH Control			
GeneID (TGGT1_)	Description	IP 1	IP 2	IP 1	IP 2	Enrichment	Rank
254470	MYR1	111	121	0	1	65.3	1
228170	**GRA44**	**55**	**37**	**0**	**0**	**35.4**	**2**
264660	**CST1**	**47**	**29**	**0**	**0**	**29.4**	**3**
204340	**Hypothetical**	**48**	**27**	**0**	**0**	**29.1**	**4**
211460	**Hypothetical**	**40**	**27**	**0**	**0**	**26.0**	**5**
270320	**PPM3C**	**36**	**27**	**0**	**0**	**24.4**	**6**
319340	**GRA52**	**33**	**23**	**0**	**0**	**21.8**	**7**
270240	MAG1	44	32	0	2	21.4	8
258458	Hypothetical	30	21	0	0	19.9	9
304955	PPM11C	27	17	0	0	17.3	10
294200	G6PDH	21	16	0	0	14.6	11
229480	TgERC	29	15	0	1	14.5	12
233870	Hypothetical	19	17	0	0	14.2	13
237500	PPM3A	19	16	0	0	13.9	14
203600	GRA50	19	16	0	0	13.9	15
279100	**MAF1a**	**16**	**19**	**0**	**0**	**13.8**	**16**
203310	**GRA7**	**16**	**16**	**0**	**0**	**12.7**	**17**
208830	GRA16	17	11	0	0	11.3	18
275860	GRA12 paralog	16	12	0	0	11.3	19
299780	Hypothetical	14	14	0	0	11.2	20
231960	GRA28	13	12	0	0	10.1	21
…	…	…	…	…	…	…	…
316250	**GRA45**	**5**	**7**	**0**	**0**	**5.2**	**60**
…	…	…	…	…	…	…	…
237230	**MYR3**	**7**	**3**	**0**	**0**	**4.5**	**67**
…	…	…	…	…	…	…	…
258580	**ROP17**	**26**	**25**	**18**	**13**	**1.2**	**224**
Total MS/MS count:		*6174*	*4295*	*3694*	*1858*		

Figure 1. MYR1-3xHA immunoprecipitation identifies many MYR1-associating *Toxoplasma* proteins.

A. Schematic of MYR1 IP-MS workflow.

B. Results of IP-MS analysis. Mass spectrometry was performed on immunoprecipitated material as depicted in Fig. 1A and the number of spectral counts was determined for all identified proteins. This experiment was performed twice (IP 1 and IP 2) for both RH::MYR1-3xHA and an RHΔ*hpt* untagged control. The identified *Toxoplasma* proteins from the two experiments were ranked according to the average NSAF enrichment in the MYR1-3xHA-expressing strain relative to the untagged RH control after adding a nominal single count to all results, enabling a ratio to be determined (Enrichment and Rank). The full dataset, including associating host proteins, is presented in File S1. Displayed here are the majority *Toxoplasma* protein identifiers (TGGT1_), i.e., the proteins that contain at least half of the peptides belonging to a group of proteins that cannot be unambiguously identified by unique peptides, the descriptive name for each protein (Description), and the corresponding number of spectral counts detected (MS/MS count) for all *Toxoplasma* proteins with an average enrichment score greater than 10. Also shown are data for the proteins GRA45, MYR3, and ROP17. Genes chosen for subsequent disruption are highlighted in orange.

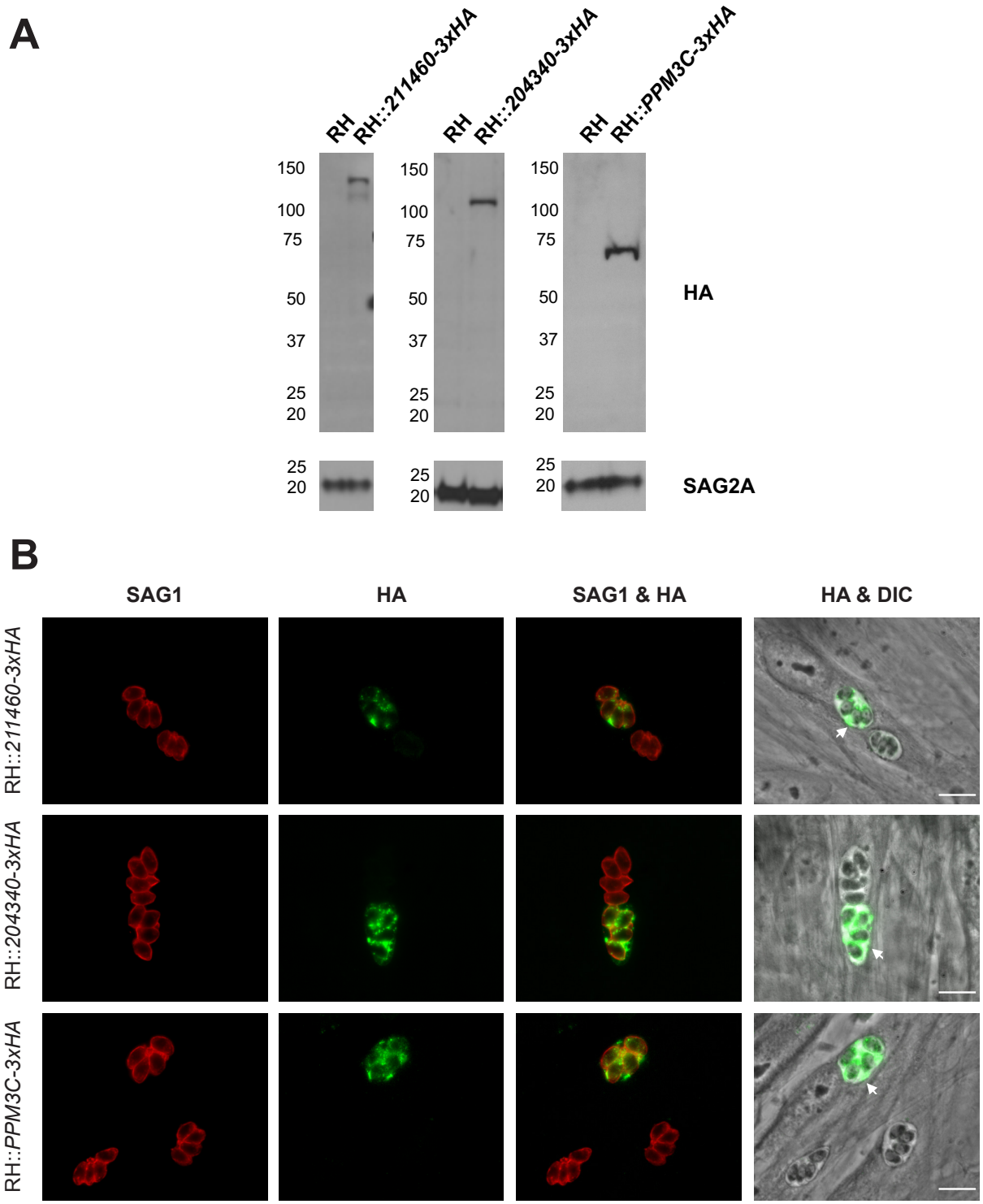

878

879 **Figure 2. 211460, 204340, and PPM3C localize to the *Toxoplasma* parasitophorous**

880 **vacuole in infected cells.**

A. Western blot of endogenously tagged parasite proteins. HFFs were infected with RHΔ*hpt*Δ*ku80* tachyzoites (RH) or with populations of RH that had been transfected with HA-tagging plasmids targeted to the indicated locus (RH::211460-3xHA, RH::204340-3xHA, and RH::PPM3C-3xHA). Lysates from infected HFFs were prepared and the HA-tagged proteins were detected by western blotting and probing with rat anti-HA antibodies. Rabbit anti-SAG2A staining was used as a loading control for total parasite protein. Approximate migration of a ladder of size standards (sizes in kDa) is indicated.

B. Representative immunofluorescence microscopy images of endogenously tagged parasite proteins. The populations of endogenously tagged parasites analyzed in Fig. 2A were allowed to infect HFFs for 16 hours before the infected monolayers were fixed with methanol. The corresponding tagged proteins in parasites that had successfully incorporated the HA-tag were detected with rat anti-HA antibodies, while all tachyzoites were detected with mouse anti-SAG1 antibodies and the entire monolayer was visualized with differential interference microscopy (DIC). The arrows indicate localization of the endogenously tagged proteins outside of the parasites and within the PV. Scale bar is 10μm.

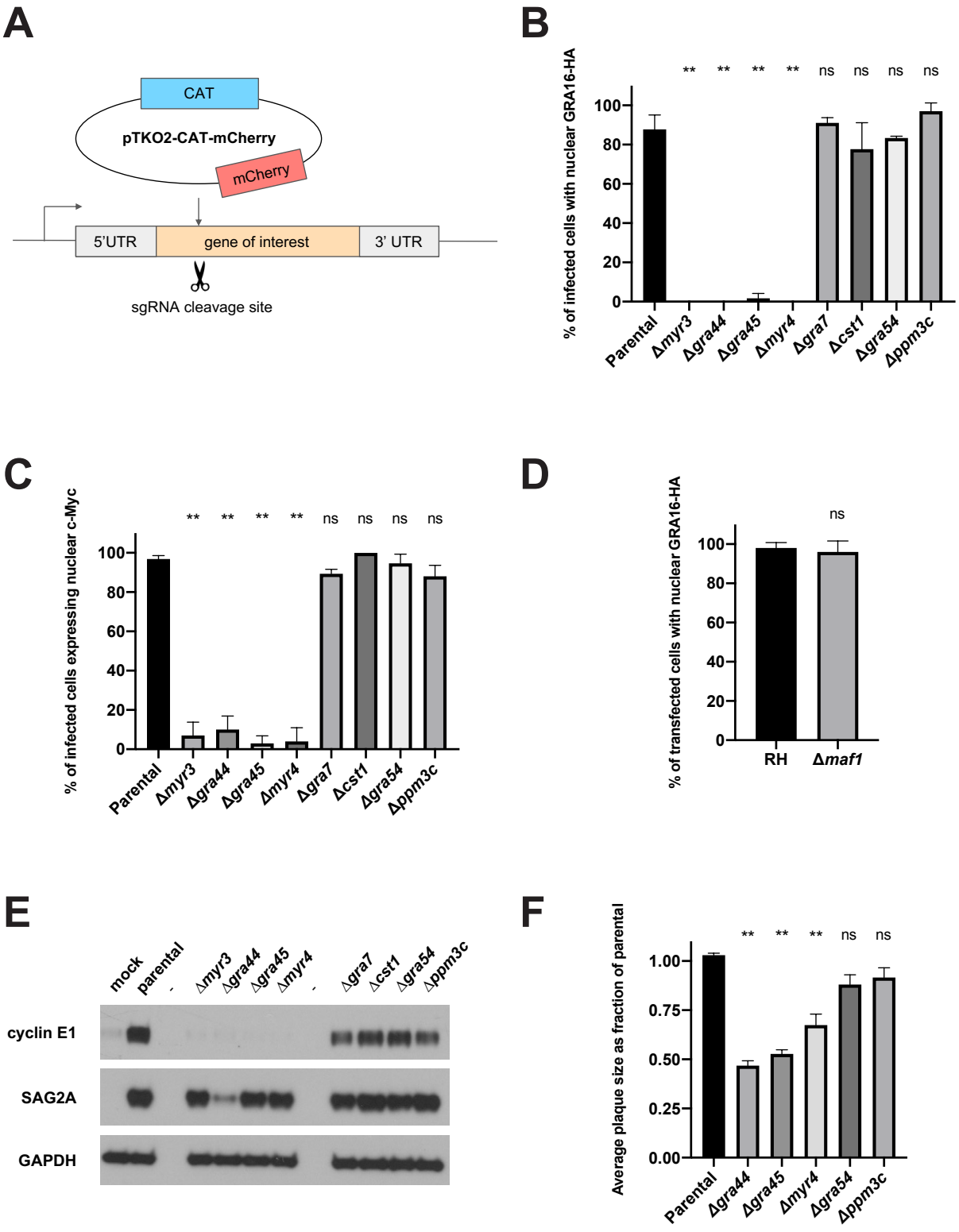

Figure 3. GRA44, GRA45, and MYR4 are required for *Toxoplasma* effector translocation and fully efficient growth *in vitro*.

A. Schematic of CRISPR-mediated gene disruption of candidate genes followed by insertion of the pTKO2 plasmid carrying *mCherry* and a *chloramphenicol acetyl transferase* (*CAT*) gene for selection in chloramphenicol.

B. Quantification of the percentage of infected cells showing GRA16-HA in the host nucleus via IFA. Tachyzoites were allowed to infect HFFs for 16 hours before the infected monolayers were fixed with methanol and stained with rat anti-HA antibodies. The averages are based on examination of at least 25 infected host cells per experiment from 2-5 biological replicates, and error bars indicate the standard deviation (SD). Statistics were performed using one-way ANOVA and Dunnett's multiple comparisons test. ** indicates $p<0.0001$ and ns indicates nonsignificance ($p>0.05$) for the indicated strain relative to the parental control.

C. Quantification of the percentage of infected cells showing upregulation of human c-Myc protein in the host nucleus via IFA. Tachyzoites were allowed to infect HFFs in serum-free media for 20 hours before the infected monolayers were fixed with methanol and stained with rabbit anti-c-Myc antibodies. Scoring and statistics are as for Fig. 3B.

D. Quantification of the percentage of transfected, infected cells showing GRA16-HA in the host nucleus via IFA. Wild-type RHΔ*hpt* and RHΔ*maf1* tachyzoites were transiently transfected with a plasmid expressing GRA16-HA, and transfected parasites were allowed to infect HFFs for 16 hours before the infected monolayers were fixed with methanol and stained with rat anti-HA antibodies. The averages are based on the examination of 25 vacuoles from 2 biological replicates, and error bars indicate the SD. Statistics are as for Fig. 3B.

925 E. Western blot of human cyclin E1 protein in infected cells. HFFs were infected with
926 the indicated tachyzoites, or mock-treated with uninfected HFF lysate, for 18 hours
927 before lysates were generated for immunoblotting. Lysates were analyzed by
928 western blotting using mouse anti-cyclin E1 antibodies. Rabbit anti-SAG2A and
929 mouse anti-GAPDH were used to assess the levels of parasite and host protein in
930 the lysate respectively. "-" indicates empty lanes.
931 F. Quantification of plaque size. HFFs were infected with tachyzoites of the indicated
932 strain for 7 days, fixed with methanol, and then stained with crystal violet. Plaque
933 size was measured using ImageJ. Plaque areas were normalized to the median of
934 the parental strain for each biological replicate. The averages are based on the
935 results of at least 3 independent biological replicates, each with 2-3 technical
936 replicates, and error bars represent the standard error of the mean. Statistics are as
937 for Fig. 3B.
938

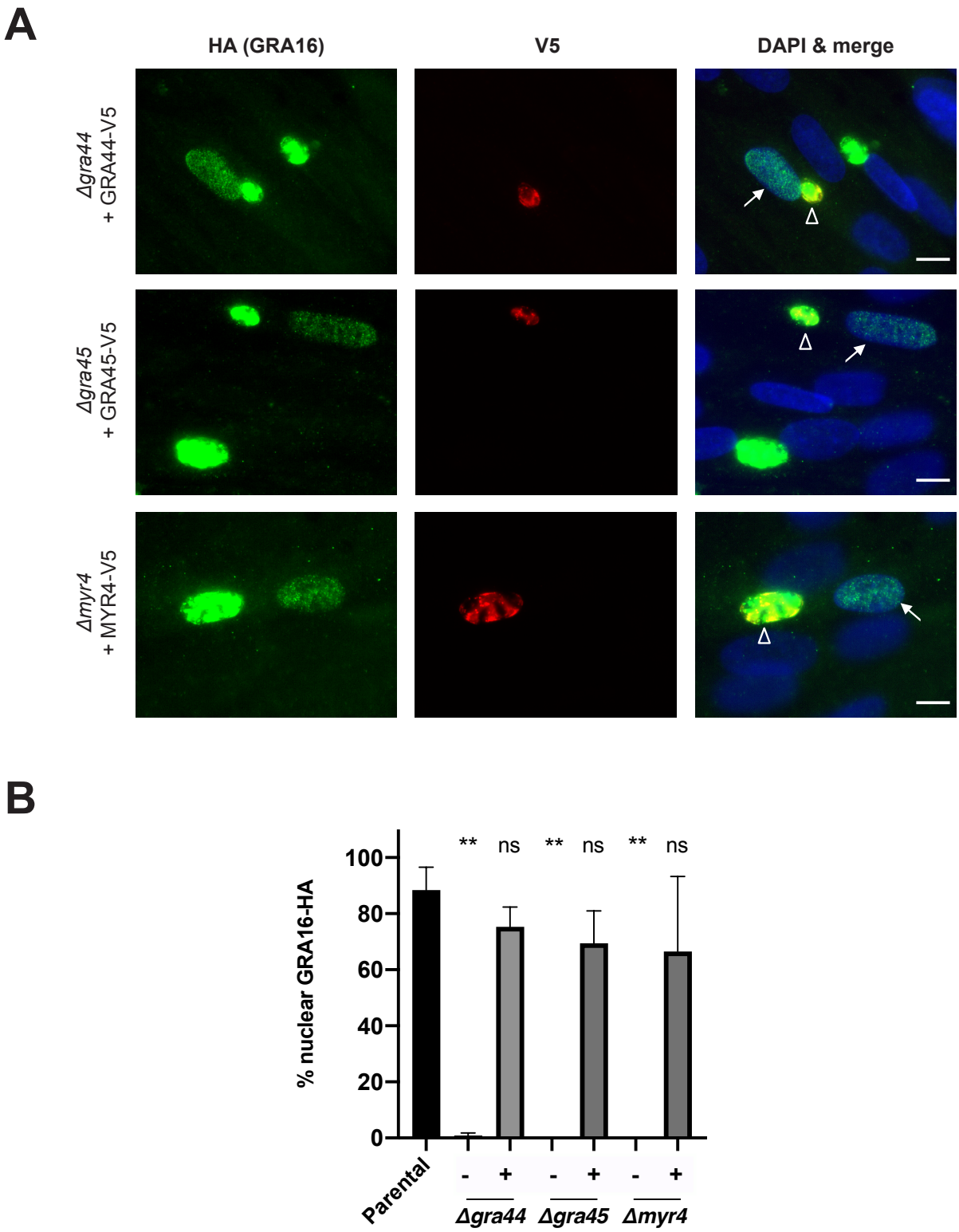

939

940 **Figure 4. Ectopic protein expression rescues the effector translocation defect in**

941 **Δ*gra44*, Δ*gra45*, and Δ*myr4* parasites.**

A. Representative immunofluorescence microscopy images of transiently expressed GRA44, GRA45, and MYR4 proteins. The indicated strains were transiently transfected with plasmids expressing the corresponding, C-terminally V5-tagged protein under its native promoter and the tachyzoites were allowed to infect HFFs for 18-22 hours before the infected monolayers were fixed with methanol. Localization of the V5-tagged proteins and rescue of the GRA16-HA host nuclear translocation were assessed by IFA using mouse anti-V5 and rat anti-HA antibodies, respectively. White arrows indicate a GRA16-HA positive host nucleus in a cell infected with tachyzoites expressing the indicated V5 tagged protein (white open arrowheads). Scale bar is 10μm.

B. Quantification of the data represented in Fig. 4A showing the percentage of infected cells showing GRA16-HA in the host nucleus via IFA. The indicated strains were transiently transfected with either empty plasmid (-) or plasmids expressing the corresponding C-terminally V5-tagged protein (+) under its native promoter. Scoring and statistics are as for Fig. 3B, except for “+” conditions where only cells infected with V5-positive vacuoles were quantified.

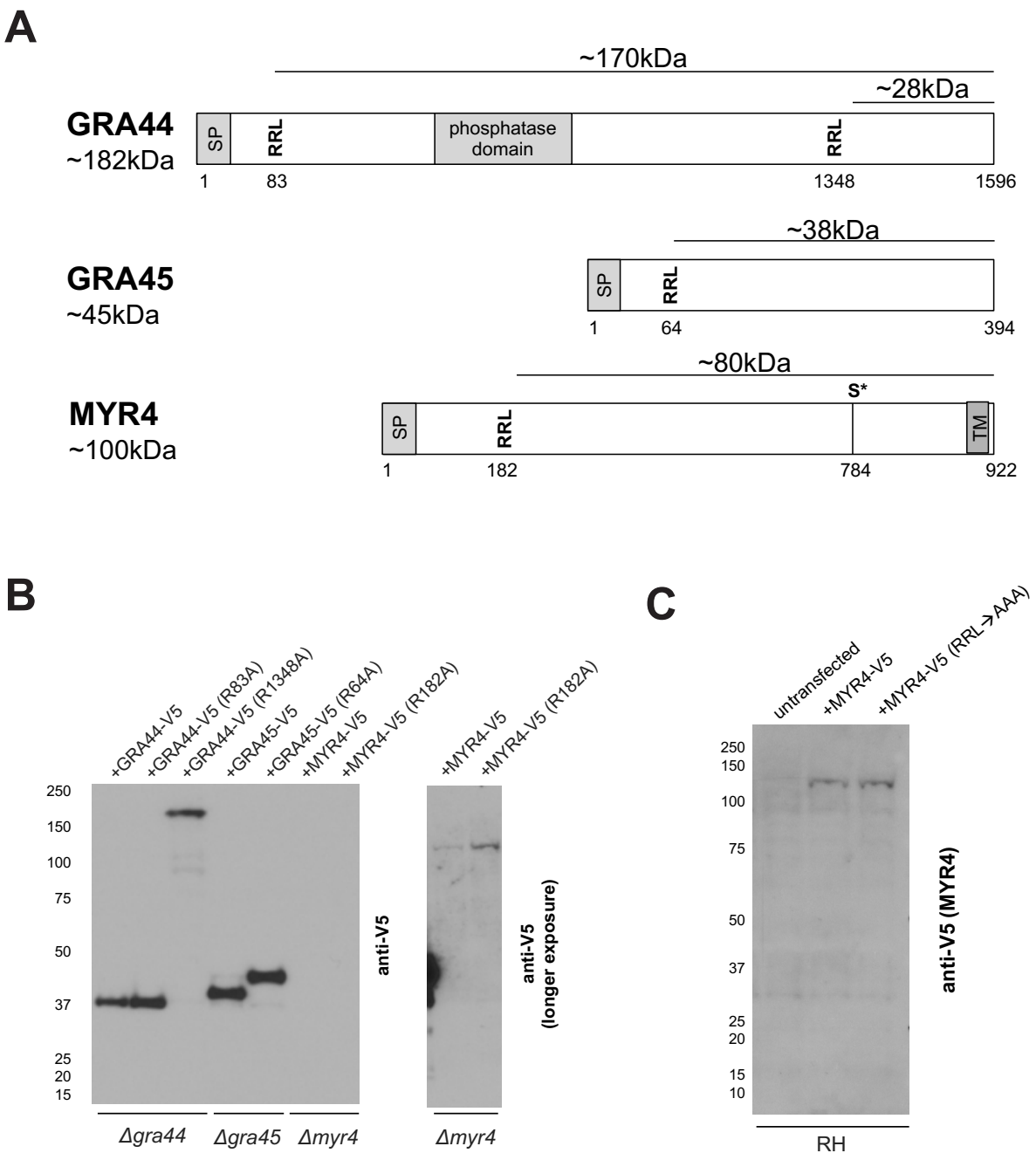

Figure 5. GRA44 and GRA45, but not MYR4, show evidence for processing at RRL sites.

A. Schematic of GRA44, GRA45, and MYR4 protein sequence showing the location of predicted signal peptides (SP), RRL tripeptide sequences, previously identified phosphorylated serine residues (S*) and conserved domains, numbered in amino

964 acid residues relative to the predicted N-terminus of the primary translation product.
965 Approximate molecular weights (kDa) of the indicated portions are indicated. The
966 amino acid sequence of MYR4 was determined using the 4th in-frame methionine
967 relative to the protein predicted in ToxoDB (v45). Transmembrane domain prediction
968 based on Phobius (Lukas Kall et al., Nucleic Acids Res 35:W429-32, 2007,
969 https://doi.org/10.1093/nar/gkm256).

970 B. Western blot of protein processing. The indicated parasite lines were transiently
971 transfected with plasmids expressing C-terminally V5-tagged versions of either the
972 indicated wildtype protein or a mutant version with the indicated RRL mutated to
973 ARL (numbers indicate the amino acid position of the mutated arginine). These were
974 then used to infect HFFs for 18 hours. Lysates were analyzed by western blotting
975 using mouse anti-V5 antibodies to detect the C-terminally V5-tagged portions of
976 each protein. Approximate migration of a ladder of size standards (sizes in kDa) is
977 indicated. The right panel is a longer exposure of the right-most two lanes of the left
978 panel.

979 C. Western blot of MYR4 processing. RHΔ*hpt* (RH) parasites were transiently
980 transfected with either WT or an RRL→AAA mutated version of C-terminally V5-
981 tagged MYR4 and allowed to infect HFFs for 24 hours before lysates were
982 generated for immunoblotting. Lysates were analyzed by western blotting using
983 mouse anti-V5 antibodies to detect MYR4. Approximate migration of a ladder of size
984 standards (sizes in kDa) is indicated.

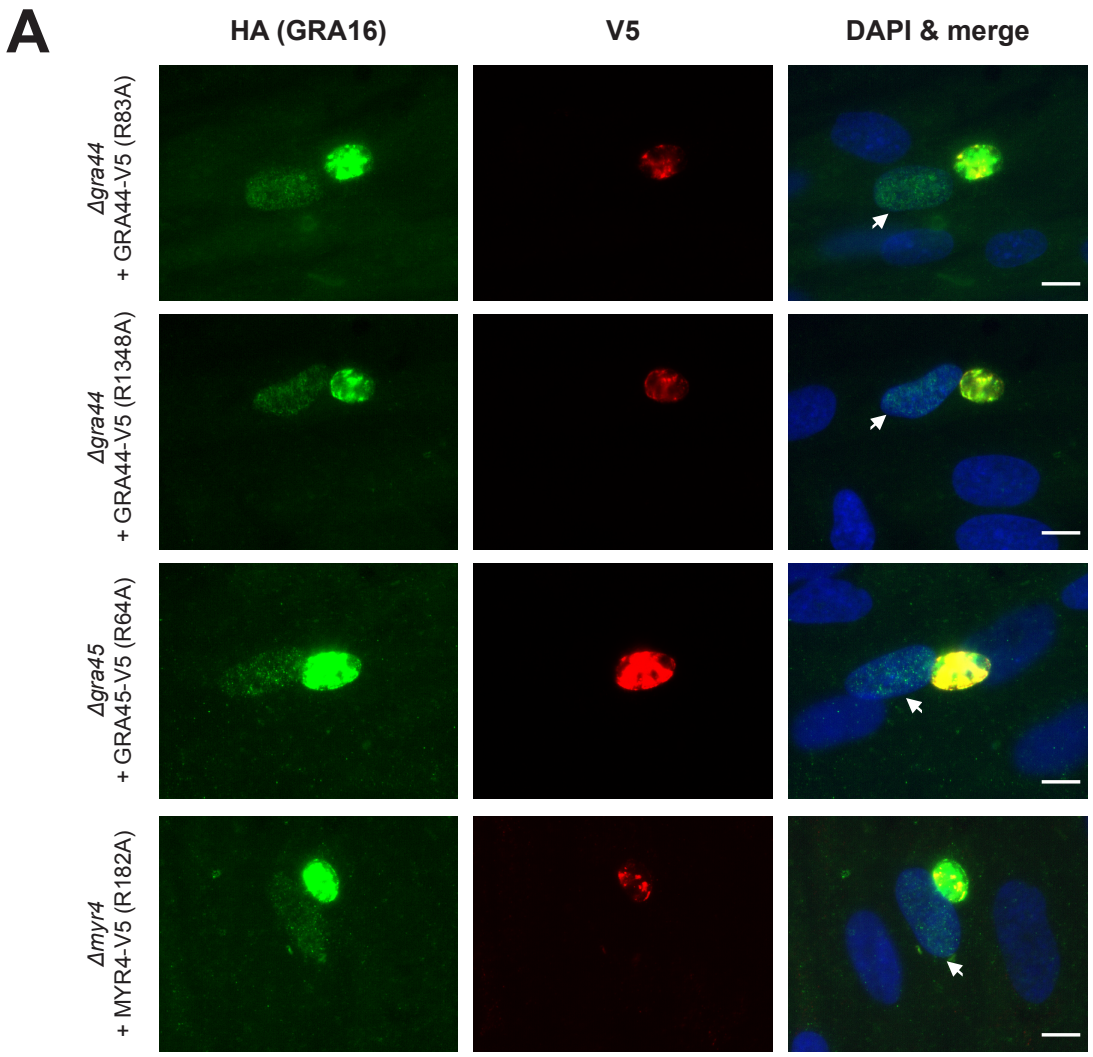

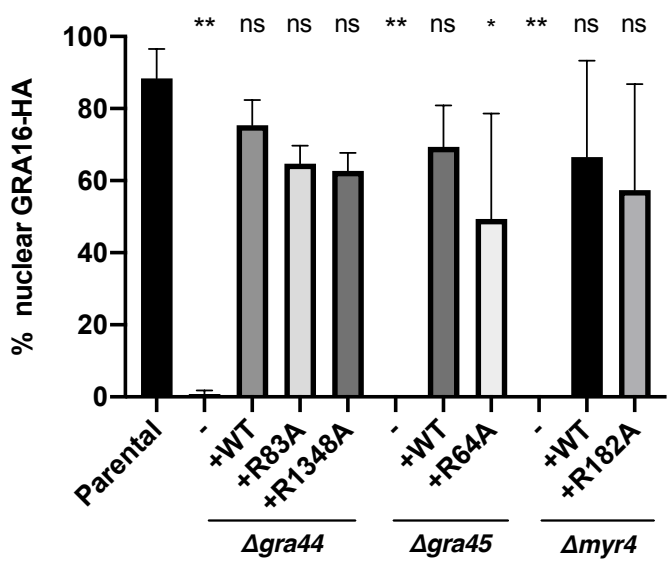

985

Figure 6. Ectopic expression of RRL mutants of GRA44, GRA45, and MYR4 rescues the translocation defect in Δ*gra44*, Δ*gra45*, and Δ*myr4* parasites.

A. Representative immunofluorescence microscopy images of transiently expressed GRA44, GRA45, and MYR4 RRL→ARL mutated proteins. The indicated strains were transiently transfected with plasmids expressing the corresponding C-terminally V5-tagged protein under its native promoter and the tachyzoites were allowed to infect HFFs for 18-22 hours before the infected monolayers were fixed with methanol. Localization of the V5-tagged proteins and rescue of the GRA16-HA host nuclear translocation were assessed by IFA using mouse anti-V5 and rat anti-HA antibodies, respectively. White arrows indicate a GRA16-HA positive host nucleus in a cell infected with tachyzoites expressing the indicated V5 tagged protein. Scale bar is 10μm.

B. Quantification of the data represented in Fig. 6A showing the percentage of infected cells showing GRA16-HA in the host nucleus via IFA. The indicated strains were transiently transfected with either empty plasmid (-) or plasmids expressing the corresponding C-terminally V5-tagged protein (+) under its native promoter. The data for the untransfected parental strain, the empty plasmid transfected strains, and the wildtype protein transfected strains are the same as in Fig. 4B and are included here for ease of comparison. Scoring and statistics are as for Fig. 4B except * indicates p=0.017.